The Journal of Foot & Ankle Surgery 58 (2019) 1138–1144

Contents lists available at ScienceDirect

The Journal of Foot & Ankle Surgery

journal homepage: www.jfas.org

Biomechanical Comparison of Locking Plate and Cancellous Screw Techniques in Medial Malleolar Fractures: A Finite Element Analysis

Dajun Jiang, MD[1,2], Shi Zhan, ME[3,4], Qing Wang, MD[1], Ming Ling, MD[1,2], Hai Hu, MD, PhD[1,2], Weitao Jia, MD, PhD[1]

[1] Surgeon, Department of Orthopedic Surgery, Shanghai Jiaotong University Affiliated Sixth People's Hospital, Shanghai, P.R. China
[2] Surgeon, Orthopedic Biomechanical Laboratory, Shanghai Jiaotong University Affiliated Sixth People's Hospital, Shanghai, P.R. China
[3] Associate Registrar, Department of Orthopedic Surgery, Shanghai Jiaotong University Affiliated Sixth People's Hospital, Shanghai, P.R. China
[4] Associate Registrar, Orthopedic Biomechanical Laboratory, Shanghai Jiaotong University Affiliated Sixth People's Hospital, Shanghai, P.R. China

ARTICLE INFO

Key Words:
cannulated screws
finite element analysis
locking compression plate
medial malleolar fracture

ABSTRACT

As the commonly used fixation strategy of medial malleolar fractures, cancellous screws (CS) have been challenged for instability, bone destruction, and metal prominence. It is still unclear whether a locking compression plate (LCP) is a better choice in such fractures. Our purpose is to compare the mechanical efficacy of LCP with traditional 4.0-mm CS for transverse, oblique, and vertical medial malleolar fractures by using finite element analysis. In this study, 3-dimensional models of the distal tibia were reconstructed from a computed tomography scan of a young healthy male adult. Conditions included 3 fracture lines at 30°, 60°, and 90°; 2 groups of fixation (LCP and CS); and 3 adduction loads of 300, 500, and 700 N applied to the medial malleolar joint surface. The proximal part of the tibia was fixed for all degrees of freedom. The fracture displacements of the LCP were smaller than those of CS ($p < .05$). The stiffness of the LCP constructs was much higher than that of the CS constructs, especially in the 90° fractures (490.3 versus 163.6 N/mm). The mean stress around the CS was higher than that in LCP for 60° and 90° fractures, but there was no difference for 30°. Maximal bone stress increased (19.84 to 50.86 MPa) and concentrated on cortical bone in LCP, whereas it concentrated on cancellous bone in CS. The results showed that LCP could improve stability, preventing bone destruction in oblique and vertical medial malleolar fractures. However, in transverse fractures, CS provides sufficient stability, with no need to use LCP.

Among ankle fractures, the medial malleolar fracture occurs frequently either as an isolated fracture or in combination with the lateral or posterior malleolar (1,2). Medial malleolar fracture patterns consist of 57% transverse fractures, 26% oblique fractures, and 6% vertical fractures (3). The medial malleolus plays an important role in maintaining the congruence of the ankle mortise, as it contributes to an average of 27.8% reduction in tibiotalar contact area if left untreated (4). Anatomic reduction and stable fixation of medial malleolar fractures are prerequisites for functional recovery and preventing posttraumatic arthritis. Traditionally, 2 parallel, partially threaded cancellous lag screws (4.0 mm in diameter) are most commonly used for these fractures (5) because of their minimal invasion to the surrounding tissue. However, their use has been challenged because of instability, with a nonunion rate of 20% (6), bone destruction, and metal prominence (6,7). To solve these problems, a variety of alternative techniques have been developed, including headless compression screws (6), fully threaded bicortical screws (8–10), absorbable screws (7), sled fixation (11), and buttress plates (12–15). However, these fixation strategies have been unable to solve existing problems completely. Thus, alternative fixation strategies are still needed.

Over the past several decades, the locking plate technique has been widely used in nearly all metaphysis regions (16) because it provides angular stability, which allows the load to be distributed more evenly and improves construct stability, especially in osteoporotic bones, enabling weightbearing much earlier as well as accelerating the fracture healing process. Also, the surrounding soft tissue and local blood supply can still be protected for better healing via the minimally invasive plate osteosynthesis technique. However, the primary concern is that, because the medial malleolus lacks sufficient soft tissue coverage, traditional locking plates often lead to metal prominence, which results in frequent pain and implant removal. Thus, we developed a new

Financial Disclosure: This investigation was sponsored by the National Natural Science Foundation of China (81572105, 31270996); Project introduction Shanghai Municipal Education Commission-Gaofeng Clinical Medicine Grant Support (20172026); Funding project for talent development in Shanghai (2017035); Medical Cross Youth Project of Shanghai Jiao Tong University (YG2017QN14); and Funding project of Shanghai Sixth People's Hospital (ynlc201617).

Conflict of Interest: None reported.

D. Jiang and S. Zhan are co-first authors.

Address correspondence to: Weitao Jia or Hai Hu, 600#, Yishan Road, Shanghai, 200233 China.

E-mail addresses: xmhuhai@hotmail.com (H. Hu), jiaweitao@shsmu.edu.cn (W. Jia).

1067-2516/$ - see front matter
https://doi.org/10.1053/j.jfas.2018.10.005

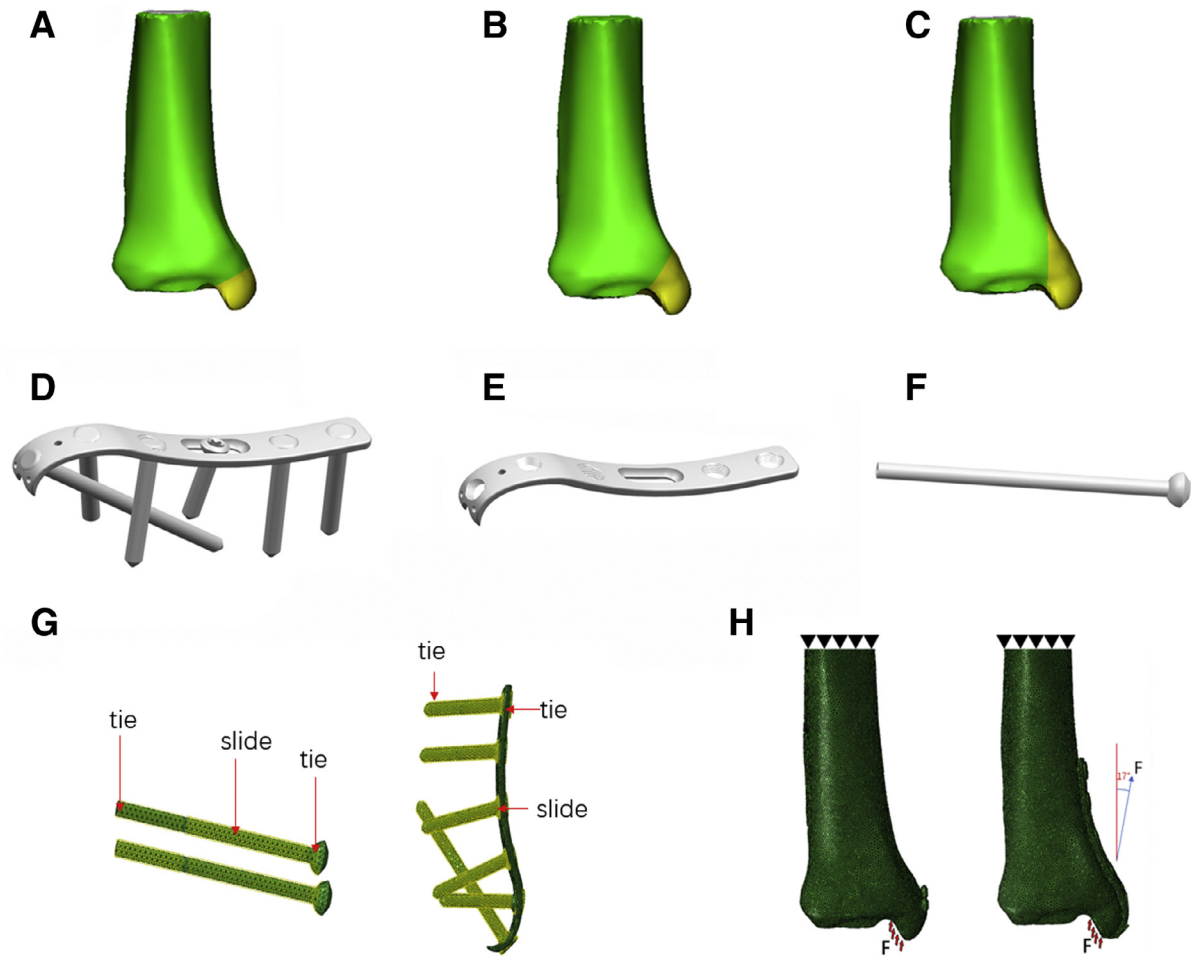

Fig. 1. Three-dimensional models of the finite element analysis. (*A–C*) Three medial malleolar fracture models with various angles of fracture lines (from left to right are 30°, 60°, and 90° fractures representing transverse, oblique, and vertical fractures). (*D* and *E*) The models of the custom-designed anatomic hook LCP used in this article. (*F*) The simplified model of the CS shown without threads. (*G*) Setting of contact surfaces. In the lag screw fixation model, the distal 1/3 part and head of the screws were tied to the bone, and the shaft of the screws was set to slide against the bone surface. In the LCP fixation model, all interactions between locking plate and screws were tied with the exception of the sliding hole. (*H*) The boundary and loading conditions. The proximal part of tibia was fixed in all degrees of freedom, and the adduction load was applied in a vice tilted at 17° in the coronal plane. Abbreviations: CS, cancellous screw; LCP, locking compression plate.

anatomical hook locking compression plate (LCP) especially for medial malleolar fractures, with the following characteristics (Fig. 1): 1) the distal part of the plate was attenuated to 1 mm in thickness to minimize implant prominence; 2) 2 barbs at the distal edge were designed to facilitate intraoperative localization; and 3) several Kirschner wire holes were set for temporary fixation and fixing tiny fracture fragments.

The aim of this study was to compare the biomechanical efficacy of the custom-designed LCP with 2 parallel cancellous screws (CS) for transverse, oblique, and vertical medial malleolar fractures via finite element analysis.

Materials and Methods

Three-Dimensional (3D) Models

A healthy young male (age 25, height 173 cm, body weight 70 kg) without a history of ankle injury was scanned using a 320-slice computed tomography scanner (Siemens, Munich, Germany) with a slicing distance of 0.625 mm from 20 cm above the ankle to the sole of the foot. Informed consent was obtained. These images, in DICOM format, were imported into Mimics 19.0 software (Materialise, Leuven, Belgium). A threshold of 662 Hounsfield units was established to differentiate between cortical and cancellous tibia bone. Then, a region of interest was selected with the region-growing method, and masks were subsequently edited to smooth the models. Finally, 3D models were established to mimic the surface geometry of the cortical and cancellous tibia, respectively.

The 3D models in STL binary format were then imported into Geomagic Studio 2012 software (Geomagic, Morrisville, NC). Fracture lines were created by planes, starting at the shoulder of the medial malleolar ankle mortise, with an angle of 30°, 60°, and 90° in the horizontal plane. These imitated transverse, oblique, and vertical medial fractures, respectively (Fig. 1*A–C*). There was no gap between fracture fragments, which mimics ideal anatomic reduction during operation.

The LCP was designed and modified using UG10.0 software (Siemens PLM Software), and the cancellous cannulated screws were created using SolidWorks2017 (DS SolidWorks Corp., Waltham, MA) according to the standard of Depuy-Synthes (West Chester, PA) (Fig. 1*D–F*).

The custom-designed locking plate was 80 mm in length and 10 mm in width. Its thickness was 2.3 mm at the proximal edge and 1.0 mm around the region of the medial malleolus. The 3.5-mm locking screws ranged from 30 to 55 mm in length fully threaded, and the 4.0-mm cancellous lag screws were 40 mm in length, 1/3 partial threaded. Note that the thread of the lag screws was simplified with little impact on the results according to a previous article (17).

The implants and these fracture models were assembled and Boolean subtracted via 3-Matic 19.0 software (Materialise) which finally generated internal fixation models of fractures as created above. All assemblies were meshed and modified in Hypermesh 13.0 (Altair Engineering, Troy, MI) to 1-mm equal-sized facets and were then converted to 4-node linear tetrahedron structural solid elements. The solid models in INP format were exported into Abaqus 6.13 (Simulia Corp., Providence, RI).

Finite Element Model

A finite element model of the intact distal tibia was composed of 37,080 nodes and 74,143 elements. All bone and implant models were assumed to have linear elastic properties. Cortical and cancellous bone was assigned as Young's modulus (E) of 7300 MPa (18,19) and 1100 MPa (20), and the Poisson's ratio was 0.3 (18,19) and 0.26 (20), respectively. The material of all fixators was assumed as titanium (Ti-6L-4V), which is the most commonly used clinically, with a Young's modulus (E) of 110,000 MPa and Poisson's ratio of 0.3 (21,22).

Interaction types of fixations were selected discreetly and logically for better simulation of real biomechanical conditions. There were 10 contact interactions overall in each lag screw fixation model, and 26 in the plate fixation model. The tie interaction between locking screws and bone was used to mimic the holding force provided by the screw

thread. In LCP fixation models, all interactions between the locking plate and screws were tied to fulfill the biomechanical mode, except for the sliding hole (Fig. 1*G*). In CS fixation models, the distal 1/3 part and head of the screw were tied to the bone, and the shaft of the screw was set to slide against the bone surface to mimic the mechanical nature of lag screw. The fiction coefficient was assigned to 0.46 for bone–bone interactions, 0.23 for implant–implant interactions, and 0.3 for bone–implant interactions (23).

In this study, all models were tested in conditions when 3 kinds of adduction loads were applied, following what the previous biomechanical experiments suggested (12–14). These loads were all set in a vice tilted at 17° in the coronal plane heading to the inferior-lateral joint surface of the medial malleolus uniformly (Fig. 1*H*). The proximal tibia was fixed in all 6 degrees of freedom for simulating a biomechanical test.

Finite Element Analysis

The stress and displacement values of each element were extracted from Abaqus software. Statistical analysis was performed using SPSS 22 (SPSS, Chicago, IL), using $p < .05$ as the threshold for significance. The normality of the displacement data was first tested by using a Kolmogorov–Smirnov test and Q-Q plot. A univariate analysis was executed to explore the differences among the factors. Furthermore, an ordinary least squares regression analysis of adduction load and the displacement of the applying node was performed, and the slope was regarded as the stiffness of the 2 internal fixation models. In addition, 2 mm of displacement was defined as failure of internal fixation.

Results

Displacement Distribution

The displacement values of the area of the fracture surface were significantly smaller in all fracture types in the LCP groups in comparison with the CS group ($p < .05$, Table 1) and showed a linear increase with the growth of loading (Fig. 2*A*), which is most obvious in the 90° fracture (Fig. 2*B*).

Table 1
Maximum (mean) displacement value in the area of fracture surface

Internal Fixation	Adduction Load	30° (mm)	60° (mm)	90° (mm)
LCP	300	0.536 (0.503)	0.519 (0.452)	0.589 (0.440)
	500	0.897 (0.844)	0.871 (0.762)	0.987 (0.738)
	700	1.258 (1.185)	1.226 (1.069)	1.391 (1.040)
CS	300	0.573 (0.542)	0.626 (0.531)	1.544 (1.183)
	500	0.960 (0.962)	1.050 (0.896)	2.620 (2.005)
	700	1.354 (1.281)	1.479 (1.254)	3.734 (2.857)
p Value		0.000*	0.000*	0.000*

Abbreviations: CS, cancellous screw; LCP, locking compression plate.
* $p < .005$.

The relation between adduction load and displacement of the applying node proved to be a linear regression ($p < .05$). The stiffness of the internal fixation models was assigned to the slope of the ordinary least squares regression line (Fig. 2*C*), which reveals that the LCP construct was stiffer than the CS construct in all 3 fracture types. Moreover, the greatest disparity was found in 90°, where the stiffness of the LCP construct was 3 times that of the CS construct. Failure loads were 1001.80, 936.346, and 346.85 N for CS fixation and 1086.7, 1116.5, and 987.5 N for LCP fixation in 30°, 60°, and 90° fractures, respectively.

Von Mises Stress Distribution

The Von Mises stress of the internal fixation in each group is shown in Fig. 3. The maximal stress values of the implants were all higher in

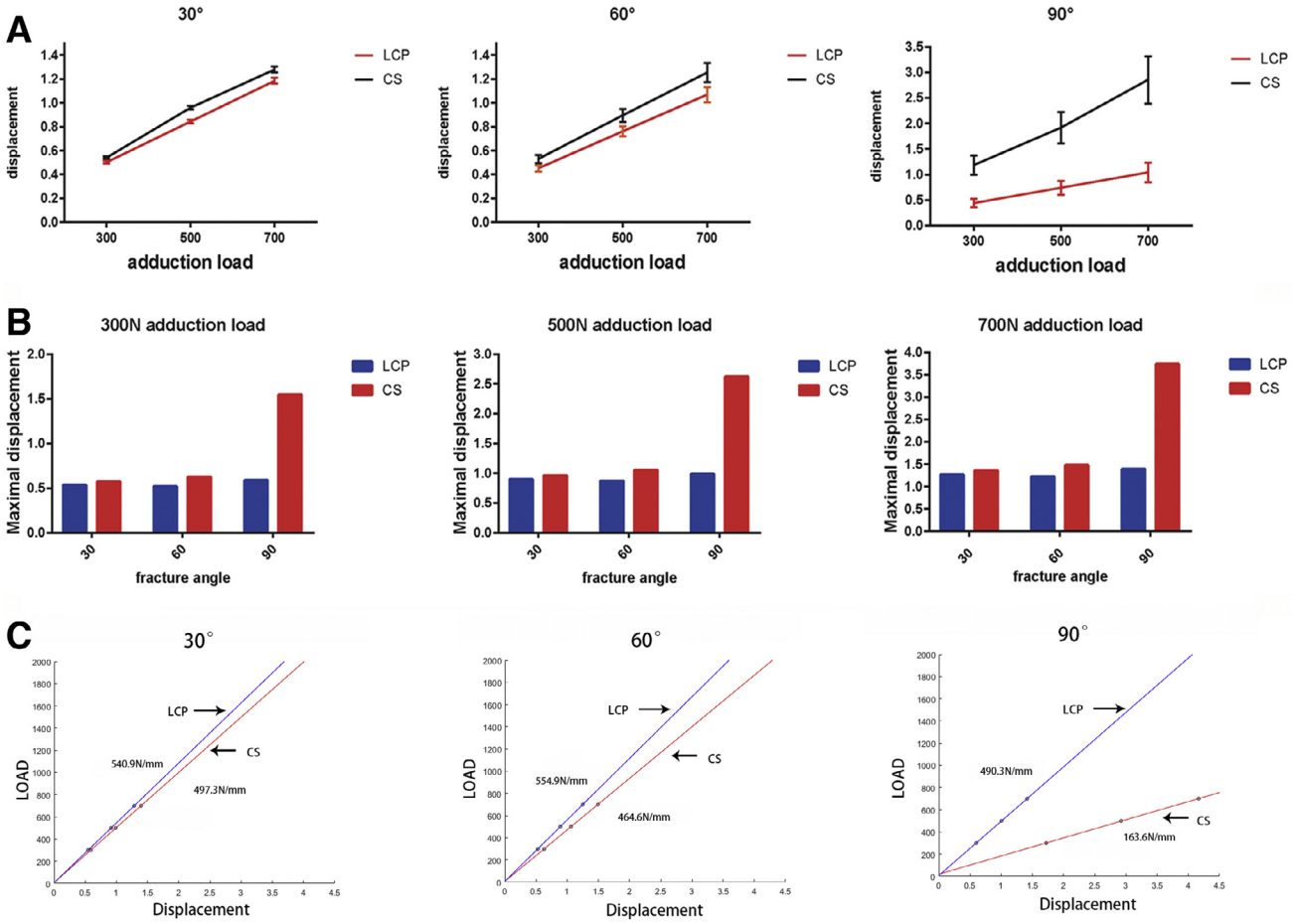

Fig. 2. Stability analysis of the implants. (*A*) The values of fracture displacement were all significantly larger in CS groups than LCP groups. (*B*) The disparity was greatest in 90° fractures. There was an increase of 0.27 to 0.53 times the peak displacement in 90° fractures compared with 60° fractures in CS groups; this increase was absent in LCP groups. (*C*) The stiffness of CS and LCP for different types of fractures. Abbreviations: CS, cancellous screw; LCP, locking compression plate.

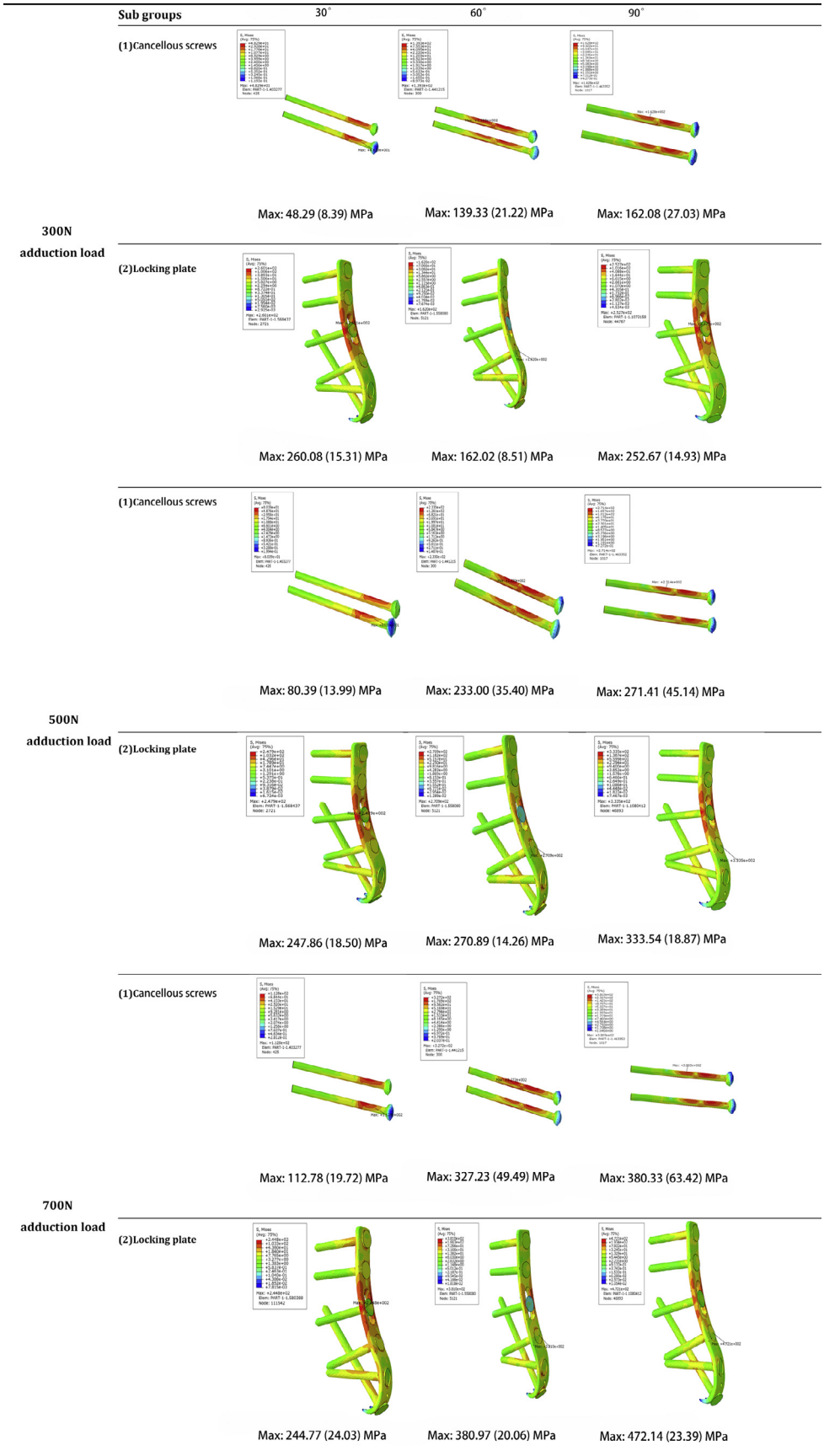

Fig. 3. Von Mises stress (VMS) distribution in the implants. In the legends, prior values indicate maximal stress, and the values in the brackets represent the mean stress of the implants.

Table 2
Maximal (mean) stress of implant and maximal stress of bone

Adduction Load	Internal Fixation	30°		60°		90°	
		Implant (MPa)	Bone (MPa)	Implant (MPa)	Bone (MPa)	Implant (MPa)	Bone (MPa)
300N	CS	48.29 (8.39)	17.14	139.33 (21.22)	18.14	162.08 (27.03)	20.85
	LCP	260.08 (15.31)	19.84	162.02 (8.51)	21.58	252.67 (14.93)	20.63
500N	CS	80.39 (13.99)	28.36	233.00 (35.40)	30.60	271.41 (45.14)	33.92
	LCP	247.86 (18.50)	33.41	270.89 (14.26)	36.15	333.54 (18.87)	35.06
700N	CS	112.78 (19.72)	39.85	327.23 (49.49)	42.06	380.33 (63.42)	46.90
	LCP	244.77 (24.03)	47.12	380.97 (20.06)	50.86	472.14 (23.39)	49.34

Abbreviations: CS, cancellous screw; LCP, locking compression plate.

the LCP groups, located at the proximal plate site, where the holes and screws interacted, and the middle segment (curative) of the plate, which clung to the cortex of the medial distal tibia. However, the mean stress of the LCP was much smaller than the maximal stress. The difference between the LCP and CS groups was the most obvious at 30° but was similar at 60° and 90° with increasing load (Table 2). In the CS group, stress was concentrated merely in areas around fractures, which were cancellous bone (Fig. 3), and it was much smaller at 30° in comparison with that at 60° and 90° (Table 2).

The mean stresses of the tibia bone around all screws in the 2 fixation groups were depicted as well (Fig. 4). The mean stresses were similar in 30° for both fixation groups, whereas the mean stresses around the screws in the CS groups were 1.32 to 2.08 times that of the LCP groups in 60° and up to 2.27 to 3.19 times that in 90°.

As to the maximal stress of the medial distal tibia bone, it ranged from 17.14 to 46.9 MPa in the CS group and from 19.84 to 50.86 MPa in the LCP groups (Table 2). The maximal stress was the highest in 60° instead of 90° in the LCP groups, whereas it increased linearly with increasing fracture line in the CS group. Moreover, there was a significant stress concentration beneath the screws in the CS group, which was at high risk of yielding (Fig. 5). Note that another maximal stress of the tibia bone in the LCP group was observed in the proximal tibia cortex, which was in contact with the proximal plate end.

Validation of the FE Analysis

The finite element analysis model in this study was based on previous biomechanical tests (12–14), simulating all setups in the real experiments. In this study, the stiffness of the CS fixation in the vertical fractures was 163.6 N/mm, which was consistent with that in previous articles (110 to 200 N/mm) (13,14), ensuring that the analysis was convincing and reliable.

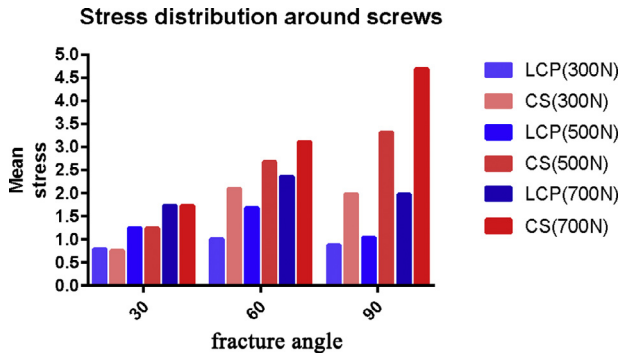

Fig. 4. Mean stresses of the tibia bone around all screws in 2 fixation groups. Mean stresses were similar in 30° for both fixation groups, whereas mean stresses around the screws in CS groups were 1.32 to 2.08 times that in LCP groups in 60°, and up to 2.27 to 3.19 times that in 90°. Abbreviations: CS, cancellous screw; LCP, locking compression plate.

Discussion

The fixation strategy for medial malleolar fractures, especially vertical fracture, is still in dispute clinically. Traditional cancellous screw fixation has well-recognized drawbacks of instability and metal prominence. A number of authors (8–10) have found that the unicortical cancellous screw, ending in the mid-metaphysis region, lacks secure purchase and increases the risks of fixation failure, especially in vertical fractures and among osteopenia patients. In addition, a 20% nonunion rate has been reported owing to fixation instability (6). In this study, the value of displacement in vertical fractures fixed with CS was remarkably high, with a failure load (causing 2 mm of displacement) merely at an estimated 346.8 N, which proves that CS are insufficient to withstand shear force in vertical fractures. Another natural defect of screw fixation is the bone-cutting effect, leading to greater risks of loosening or pullout of screws. As Fig. 5 reveals, there was a significant stress concentration beneath the CS, which may result in bone cutting in most cases.

The locking plate technique is a promising method in medial malleolar fractures, since it has been used in almost all metaphysis fractures for its advantages of biologic property, angular stability, and ability to convert shear force into compression force (16). Also, previous studies have confirmed the advantage of the stability of the plate technique in vertical fractures of the medial malleolus (13,14,24). Wegner et al (14) demonstrated that the stiffness of the construct fixed with a 4-hole antiglide plate in vertical fracture can reach as high as 463 (standard deviation 91) N/mm, which is significantly stiffer than parallel or divergent unicortical screws and bicortical screws. However, to date, no biomechanical study has been carried out to investigate the use of the locking plate in medial malleolar fractures. To compare the internal fixation of cancellous lag screws, we modified the traditional buttress plate to an anatomic hook LCP (Fig. 1) for the best customization to the medial malleolus. In this study, no stress concentration was detected on the thinning part of the plate, so there is no need to worry about breakage resulting from decreasing thickness. Similar to previous successful use of the antiglide plate, the LCP in this study exhibited surpassing stability over traditional CS as well, with significant reduction in displacement and improvement in stiffness. Note that, in vertical fractures, the stiffness of the LCP was 490.3 N/mm (Fig. 2*C*), 3 times that of CS fixation, which very closely resembles the stiffness of the antiglide plate (463 N/mm) in the study of Wegner et al (14). Moreover, we found that the LCP shared more stress than the CS, but the mean stress was much lower, owing to the advantage of dispersing stress across the implant. Nevertheless, the maximal stress of LCP in each fracture type (162.0 to 472.1 MPa) was obviously lower than the yield strength of the most commonly used Ti-6Al-4V alloy (889 to 921 MPa) (25).

The maximal and mean stress of CS was much lower than that of LCP (Fig. 3), but the decreasing stress of the implants gave no rise to fixation instability (Table 1). This contradiction reflects that in such a fracture, the adduction force more likely acts as a compression force, which contributes little to displacement rather than shear force. As a result,

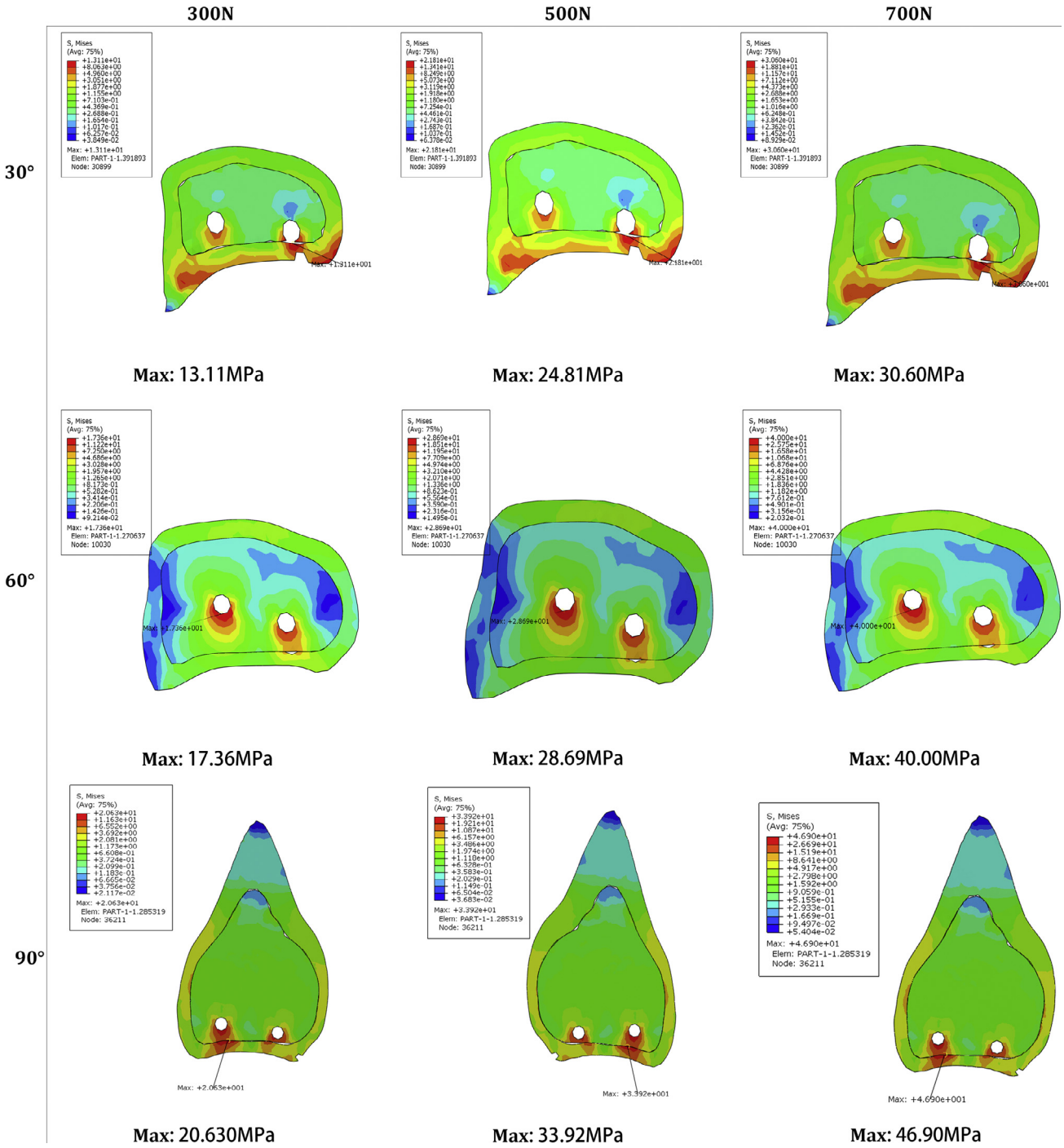

Fig. 5. Stress distribution of fracture surface in cancellous screw (CS) groups. There is a significant stress concentration beneath the screws, which is at high risk of yielding.

transferring stress from the bone to the implants is of little benefit but increases the risks of fatigue failure.

Stress was mostly concentrated in the proximal plate site, where holes and screws interacted and the plate curved, whereas it was concentrated merely in areas around fractures in CS, which caused a severe bone-cutting effect. Via analyzing the average stress around the screws, we confirmed the bone-protection effect of LCP in vertical and oblique fractures but not in transverse fractures. In consequence, patients fixed with LCP may bear weight earlier with fewer risks of bone destruction and subsequent fixation failure, thus accelerating fracture healing by improving mechanical stimulation.

There are some limitations in this study. First, there were 2 stress concentrations in LCP fixation under the loadings (one in the curvature of the plate, the other around the proximal segment of tibia) that need to be modified (e.g., elongating and slanting the proximal edge of the plate for increasing the contact area with the proximal tibia and dispersing stress concentration). Second, the material property in this model was based on a previous study (17), in which the bone was assumed to be of isotropic elastic material, whereas in reality, bone is composed of anisotropic viscoelastic material. In addition, we did not consider the yielding process in this model, which is quite severe in CS fixation, resulting in likely overestimation of the stability of CS fixation.

Third, we simplified the model without considering the fracture size or the impact of ligaments and joint capsule, and the fracture lines may be too simple in clinical reality. However, these results are enough to illustrate the differences between LCP and CS.

In conclusion, the LCP technique is promising in terms of its advantages of improving stability and preventing bone destruction in oblique and vertical medial malleolar fractures, but it is not prominent in transverse fractures. In transverse fractures, traditional 4.0-mm CS are adequate to provide stable fixation without the necessity of using the LCP technique.

Acknowledgments

The authors gratefully acknowledge Prof. Peter Shull from Shanghai Jiaotong University for his language edits and suggestions. This project could not have been performed without the support of Prof. Changqing Zhang, vice director of Shanghai Jiaotong University affiliated Sixth People's Hospital, and Prof. Yimin Chai, the head of orthopaedic department of Shanghai Jiaotong University affiliated Sixth People's Hospital.

References

1. Daly PJ, Fitzgerald RH Jr, Melton LJ, Ilstrup DM. Epidemiology of ankle fractures in Rochester, Minnesota. Acta Orthop Scand 1987;58:539–544.
2. Court-Brown CM, Caesar B. Epidemiology of adult fractures: a review. Injury 2006; 37:691.
3. Ebraheim NA, Weston JT, Ludwig T, Moral MZ, Carroll T, Liu J. The association between medial malleolar fracture geometry, injury mechanism, and syndesmotic disruption. Foot Ankle Surg 2014;20:276–280.
4. Lareau CR, Bariteau JT, Paller DJ, Koruprolu SC, Digiovanni CW. Contribution of the medial malleolus to tibiotalar joint contact characteristics. Foot Ankle Spec 2015;8:23.
5. Rudloff Matthew I. Fractures of the lower extremity. In: Canale ST, ed. *Campbell's Operative Orthopaedics*, 13th ed., Amsterdam: Elsevier, 2017:2712–2816.
6. Barnes H, Cannada LK, Watson JT. A clinical evaluation of alternative fixation techniques for medial malleolus fractures. Injury 2014;45:1365–1367.
7. Tang J, Jin-Feng HU, Guo WC, Ling YU, Zhao SH. Research and application of absorbable screw in orthopedics: a clinical review comparing PDLLA screw with metal screw in patients with simple medial malleolus fracture. Chin J Traumatol 2013;16:27–30.
8. Ricci WM, Tornetta P, Borrelli J Jr. Lag screw fixation of medial malleolar fractures: a biomechanical, radiographic, and clinical comparison of unicortical partially threaded lag screws and bicortical fully threaded lag screws. J Orthop Trauma 2012;26:602–606.
9. King CM, Cobb M, Collman DR, Lagaay PM, Pollard JD. Bicortical fixation of medial malleolar fractures: a review of 23 cases at risk for complicated bone healing. J Foot Ankle Surg 2012;51:39–44.
10. Fowler TT, Pugh KJ, Litsky AS, Taylor BC, French BG. Medial malleolar fractures: a biomechanical study of fixation techniques. Orthopedics 2011;34:349–355.
11. Wegner AM, Wolinsky PR, Cheng RZ, Robbins MA, Garcia TC, Amanatullah DF. Sled fixation for horizontal medial malleolus fractures. Clin Biomech 2017;42:92–96.
12. Toolan BC, Koval KJ, Kummer FJ, Sanders R, Zuckerman JD. Vertical shear fractures of the medial malleolus: a biomechanical study of five internal fixation techniques. Foot Ankle Int 1994;15:483.
13. Dumigan RM, Bronson DG, Early JS. Analysis of fixation methods for vertical shear fractures of the medial malleolus. J Orthop Trauma 2006;20:687–691.
14. Wegner AM, Wolinsky PR, Robbins MA, Garcia TC, Maitra S, Amanatullah DF. Antiglide plating of vertical medial malleolus fractures provides stiffer initial fixation than bicortical or unicortical screw fixation. Clin Biomech 2015;31:29.
15. Jones DA, Cannada LK, Bledsoe JG. Are hook plates advantageous compared to antiglide plates for vertical shear malleolar fractures? Am J Orthop 2016;45:E98.
16. Christoph Sommer. Locking plates. In: Rüedi TP, Murphy WM, eds. *AO Principles of Fracture Management*, 3rd ed., Stuttgart, Germany: Thieme, 2017:269–308.
17. Anwar A, Lv D, Zhao Z, Zhang Z, Lu M, Nazir MU, et al. Finite element analysis of the three different posterior malleolus fixation strategies in relation to different fracture sizes. Injury 2017;48:825–832.
18. Nakamura S, Crowninshield RD, Cooper RR. An analysis of soft tissue loading in the foot—a preliminary report. Bull Prosthet Res 1981;14:27–34.
19. Qiu TX, Teo EC, Yan YB, Lei W. Finite element modeling of a 3D coupled foot-boot model. Med Eng Phys 2011;33:1228–1233.
20. Kim HJ, Kim SH, Chang SH. Bio-mechanical analysis of a fractured tibia with composite bone plates according to the diaphyseal oblique fracture angle. Compos B Eng 2011;42:666–674.
21. Fan Y, Xiu K, Duan H, Zhang M. Biomechanical and histological evaluation of the application of biodegradable poly-l-lactic cushion to the plate internal fixation for bone fracture healing. Clin Biomech 2008;23:S7–S16.
22. Benli S, Aksoy S, Havitcioğlu H, Kucuk M. Evaluation of bone plate with low-stiffness material in terms of stress distribution. J Biomech 2008;41:3229–3235.
23. Eberle S, Gerber C, Von OG, Högel F, Augat P. A biomechanical evaluation of orthopaedic implants for hip fractures by finite element analysis and in-vitro tests. Proc Inst Mech Eng H J Eng Med 2010;224:1141–1152.
24. Blake S, Yakubek G, Shaer J. Use of a locked fibular plate for fixation of a vertical shear medial malleolus fracture: a case report. J Foot Ankle Surg 2015;54:1202–1205.
25. Yang D, Liu Z. Quantification of microstructural features and prediction of mechanical properties of a dual-phase Ti-6Al-4V alloy. Materials 2016;9:628.